Hindawi
Geofluids
Volume 2019, Article ID 7287438, 11 pages
https://doi.org/10.1155/2019/7287438

Research Article

Experimental Study on Damage and Gas Migration Characteristics of Gas-Bearing Coal with Different Pore Structures under Sorption-Sudden Unloading of Methane

Gang Wang[1,2] **Yangyang Guo**[2] **Chang'ang Du**[2] **Lulu Sun**[1,2] **Zhiyuan Liu**[2] **Yue Wang**[2] **and Jianjun Cao**[3]

[1]*Mine Disaster Prevention and Control-Ministry of State Key Laboratory Breeding Base, Shandong University of Science and Technology, Qingdao 266590, China*
[2]*College of Mining and Safety Engineering, Shandong University of Science and Technology, Qingdao 266590, China*
[3]*China Coal Technology Engineering Group Chongqing Research Institute, Chongqing 400039, China*

Correspondence should be addressed to Gang Wang; gang.wang@sdust.edu.cn

Received 27 September 2018; Revised 14 November 2018; Accepted 27 November 2018; Published 11 February 2019

Academic Editor: Jaewon Jang

Coal and gas outburst is one of the most serious hazards in underground mine operations. In this paper, we explored the damage and gas seepage characteristics of gas-bearing coal samples with different pore structures under methane sorption-sudden unloading conditions using a self-developed experimental apparatus. The results show that (1) the deformation of coal samples can be divided into three stages, namely, pressure-increase-induced compression, sorption-induced expansion, and sudden-unloading-induced deformation or failure stage; (2) with the increase of the number of diffusion pores in the coal sample, the amount of gas sorption gradually increases and the expansion and failure of coal samples become more obvious; (3) in the experiment, the damage of coal samples is mainly along the axial direction and rarely along the radial direction; (4) the radial strain is always greater than the axial strain.

1. Introduction

Coal is an important energy source for human activities and engineering applications. Many factors could cause disaster during coal mining including coal mine gas, water, and dust. Due to complexity of mining disaster-causing mechanisms, situation for safe mining production is extremely severe [1–3]. Coal and gas outburst is an extremely complex phenomenon of dynamic instability occurring in coal mines. Although the frequency of coal and gas outburst has decreased in recent years with the development of technology and the improvement of mining methods, coal and gas outburst is still regarded as one of the most serious hazards in mine operations [4–7]. Due to the complexity of coal and gas outburst mechanisms, more and more researches accepted the hypothesis that coal and gas outburst is the result of the combined effects of geological structure, gas migration, and the nature of coal samples [8–13].

Gas sorption-desorption is a major factor in the influence of coal and gas outburst. Although it is well known that coal expands when adsorbing gas and shrinks during gas desorption, the view on how gas sorption-desorption affect coal deformation is under debate (Hol et al. 2011 and [12–15]). Langmuir studied the gas sorption characteristics of solid surfaces and proposed the equation of state for monolayer sorption, namely, the Langmuir equation. Some scholars believed that coal sorption gas is more than a monolayer morphology and proposed a theoretical multilayer sorption model based on Brunauer-Emmett-Teller theory [16, 17]. According to the knowledge of surface physical chemistry, He et al. [18] believed that the gas inside the pores of coal weakens the van der Waals force of the micropores and crack surfaces, which generates expansion energy

and macroscopically leads to expansion deformation of coal. Zhou [19] believed that the deformation mechanism of gas-bearing coal is that when the coal absorbs gas, the carbon molecular spacing increases and the gas molecules open up the micropores and microcracks in the coal. Gao et al. [20] explained the mechanism of the sorption expansion behavior of coal from the molecular structure perspective. Karacan [21, 22] showed that gas-bearing coal produces a certain free volume due to the presence of gas, so that the macroscopic free molecular structure of coal can expand during the test phase. Goodman et al. [23] studied coal structure changes caused by gas sorption and diffusion. Most of the theories believe that the sorption process occurs on the surface of the adsorbent. But when the pore size of some microporous media (coal, activated carbon, etc.) is comparable to the size of the adsorbed molecules, sorption may also occur in the internal space of the adsorbent [24].

In addition, researchers have also experimentally explored the effects of gas sorption-desorption on coal deformation. Barrer [25] studied the sorption and desorption of coalbed methane in solids using natural zeolite as the adsorbent and considered that sorption and desorption are reversible processes. St. George and Barakat [26] studied the coal deformation during sorption and desorption of different gases under uniaxial pressure. Ju et al. [27] found through experiments that the desorption curve conforms to the Langmuir equation when the degree of coal deformation is low, but not when the degree of coal deformation is high. Liu et al. [28, 29] experimentally studied the swelling deformation of coal induced by gas sorption using a self-developed testing apparatus based on coal solid-gas coupled mesomechanics and discussed the dynamic process of expansion deformation due to sorption of gas under different pressures, the anisotropy of sorption deformation, and the relationship between sorption deformation value and gas sorption amount. Zhang et al. [30] studied the process of sorption and desorption of raw coal and briquette and found that the relationship between volumetric strain and time is consistent with the Langmuir equation. They also showed that the strain process can be divided into six stages for of raw coal, but only three stages for briquette. However, they did not separately discuss the changes of axial strain and radial strain and neglected the influences of anisotropy to coal deformation. In fact, the variation trend of axial strain and radial strain of different coal samples under different pressures may be different. Baisheng et al. [31] qualitatively analyzed the deformation characteristics of raw gas-bearing coal samples during the whole process of sorption and found that the deformation characteristics of coal during the whole process of sorption and desorption were slightly different from those described using Langmuir equation. Liu et al. [32] analyzed the thermal deformation effects of coal sorption and desorption from the microscopic and macroscopic perspectives. Brochard et al. [33] studied the sorption behavior of methane molecules in micropores during coal sorption expansion deformation. Mahabadi et al. [34, 35] and Grozic et al. [36] explored the mechanism of gas migration and medium expansion in porous media by studying the effects of methane gas and the influence of gas generation on methane hydrate deposits such as delta deposits. Despite these studies on the sorption-desorption behavior of coal, very few studies have explored that damage characteristics of coal with damage under rapid gas unloading and redistribution.

Compared with raw coal, briquettes made at various pressures and artificially adjusted molding parameters are characteristics of easy processing and easy transportation and also conform at varying degrees to the pore-fracture model of raw coal (Figure 1), which considers that coal is rich in micropores and transition pores and gas migration sites in coal are mainly composed of pores and fissures. Therefore, they are often used as substitutes for raw coals in laboratories. In this view, studies of methane flow characteristics of pores using briquette could better interpret the laboratory phenomena and explain the mechanism of the influence of coal pore and fracture on coal and gas outburst. In this study, we utilized briquette specimens with different pore structure as the research object, carried out experiments on the differences of their deformation under sudden unloading using a self-developed experimental apparatus, analyzed the characteristics of their damage and gas migration, and further discussed the mechanism of coal and gas outburst.

2. Experimental Methods

2.1. Experimental Materials. The coal samples were taken from the no. 8 coal seam of class V failure type of Fuyang Coal Mine of Chongqing Songzao Coal and Electricity Co. Ltd., China, and prepared as briquettes as described as follows: (1) smash and sieve coal samples on a pulverizer and divide them into three types with particle sizes of 0.83–0.38 mm, 0.38–0.18 mm, and 0.18–0.12 mm, respectively; (2) weigh 225 g of the coal powder or the mixture of any two coal powders at 1 : 1 ratio and prepare them as slurry by mixing them evenly with 16 g water in a container; (3) put the slurry in the press mold and press the slurry at molding pressure of 80 kg/cm^2 to form the standard piece with diameter of 50 ± 1 mm and length of 100 ± 1 mm; (4) dry the sample in a drying box, keep them dry in a dryer, and carefully polish their end surface with a fine sandpaper to ensure that the surface sticking to the strain gauge is flat; (5) clean the polished end surface using sanitary cotton balls wetted by anhydrous ethanol, place the strain gauge to the end surface of the sample using glue 502, and stroke the gauge to flat; and (6) number the samples as C-1, C-2, C-3, C-4, and C-5, respectively, and place them in a curing box for testing. Figure 2 shows the images of the prepared samples, and Table 1 shows the characteristics of the coal samples.

2.2. Coal Sample Pore Structure Characteristic Test. The amount of gas sorption on coal is closely related to coal surface area, which is related to the pore characteristics of coal. Coal characteristics are important factors affecting the content of free gas of coal and determining coal's gas sorption, diffusion, and seepage, which are basic indicators of the permeability of coal seams. In order to understand the pore structure characteristics and pore size distribution

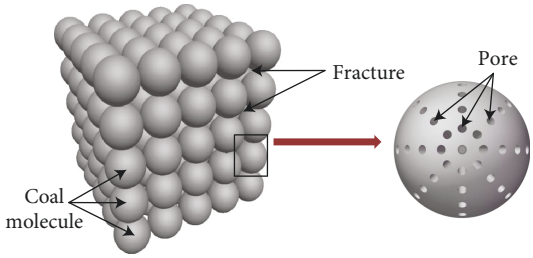

Figure 1: Schematic diagram of coal pore-fracture structure.

Figure 2: Well-prepared coal samples for experiments.

of coal samples, we measured the basic parameters of pores of coal samples using the mercury intrusion method.

As shown in Table 1, the porosity and specific surface area of the five coal samples gradually increase with the decrease of the particle size. According to the criteria for pore classification proposed by Hodort [37], these pores are divided into macropores with pore size > 1000 nm, mesopores with pore size of 100–1000 nm, transition pores with pore size of 10–100 nm, and micropores with pore size < 10 nm. In addition, according to the migration characteristics of gas in the pores of coal samples, these pores are divided into two types: diffusion pores with pore size < 100 nm and seepage pores with pore size ≥ 100 nm. Figure 3 shows the distribution of pores of the coal samples. In Figure 3, different bars represent the volumes of pores with different sizes, red points indicate the proportion of diffusion pores in the total pore volume, and blue points indicate seepage pores. It can be seen from the figure that the total pore volume is almost the same among the five coal samples, and the C-1 coal sample is rich in macropores and mesopores, while the C-5 coal sample is rich in micropores and transition pores. In addition, with the decrease of the particle size, the content of the diffusion pores increased from 46.37%, 51.23%, 56.05%, 64.02% to 65.89%, while the seepage pores decreased from C-1, C-2, C-3, C-4 to C-5.

2.3. Experimental Apparatus. A self-developed experimental apparatus for sudden unloading of gas-bearing coal was used in the study. Figure 4(a) shows the schematic of the apparatus. This apparatus consists of a pressure cell, an unloading device, a data acquisition and control system, and an inflatable system. The pressure cell is mainly composed of a coal chamber. Its two ends are fixed using flanges to form a stably sealed cavity with airtightness of 98.7%. Outside of the flange, one end of the pressure cell is equipped with a gas-filling inlet for gas loading as well as the data wires of gas pressure detector and strain gauge for monitoring experimental parameters, and the other end of the cell is connected with the gas-unloading device. The unloading device is mainly composed of 6 air outlets, 5 of which are distributed around its circumference and 1 is in the center. When all 6 solenoid valves are fully opened, 1.5 MPa gas pressure can be fully unloaded from the cavity to the atmospheric pressure within 0.02 s, which can meet the transient characteristics of coal and gas outburst. The inflatable system consists of a high-pressure gas cylinder, pressure-reducing valves, barometers, air-conducting tubes, and other components. It provides a pressure environment for the experiment. The gas can flow from the high-pressure gas cylinder, passing through pressure-reducing valves, air-conducting tubes, switch valves, and barometers to the gas-filling port. The data acquisition and control system mainly includes gas pressure detectors, strain gauges, a data acquisition instrument, a gas relief control, and a computer and its related software. The gas pressure detector has a range of 0 to 1.6 MPa and a measurement accuracy of 0.3% and can accurately monitor pressure changes in the pressure cell. The strain gauges with resistance of 120 Ω are chosen to meet the requirements of the experimental system and used to acquire the strain of gas-bearing coal on axial and radial directions during the experiment. The pressure values and strain signals acquired through both the pressure sensors and strain gauges are processed using a high-speed acquisition board, analyzed using a data acquisition instrument, and displayed and stored using the DHDAS software. The data acquisition and control system has a precision of 10^{-6} and maximum monitoring frequency of 10^4/s.

When the preset sorption time is reached, gas pressure is unloaded by opening certain numbers of solenoid valves of the gas-unloading device. The gas pressure and coal strain in the pressure cell are monitored in real-time to achieve continuous and automatic data acquisition and ensure the continuity and reliability of data measurement during the whole experimental process.

2.4. Experimental Procedure. The test uses CH_4 with a purity of 99.995% as the gas source. All coal samples are taken out from the curing box 15 minutes prior to the initiation of experimental to ensure consistent initial conditions for all coal samples.

The experiments are carried out according to the following steps. Figure 4(b)) is a schematic diagram of the device system and its operational steps. (1) Remove the coal sample from the curing box, weld the copper wire on the strain gauge (BX120-20AA) to the conditioner, and examine the resistance. If the resistance value reaches 120 Ω±0.1 Ω, proceed to the next step. (2) Place the coal sample in pressure cell, fix and seal the cell, and connect

Table 1: Proportion scheme and pore structure of coal samples used in the experiments.

Samples	Proportion scheme	Porosity (%)	Specific surface area (m^2/g)
C-1	0.38–0.83 mm, 225 g	14.58	24.40
C-2	0.38–0.83 mm, 122.5 g + 0.18–0.38 mm, 122.5 g	15.63	25.02
C-3	0.18–0.38 mm, 225 g	15.87	26.16
C-4	0.18–0.38 mm, 122.5 g + 0.12–0.18 mm, 122.5 g	16.09	27.64
C-5	0.18–0.12 mm, 225 g	16.52	29.35

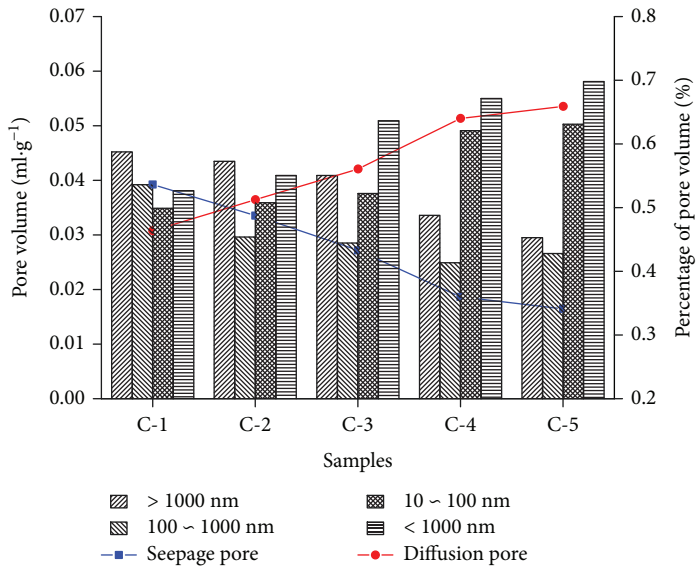

Figure 3: The pore distribution of coal samples.

the pressure sensor to the cell. (3) Measure the air pressure in the cell and open the vacuum pump to evacuate the pressure cell. (4) Open the inlet valve and inject CH_4 gas into the pressure cell. After reaching the preset pressure of 1.5 MPa, vacuum again to avoid the influence of impurity gases on the experimental results. (5) Turn on the monitoring and control system to monitor changes of coal strain and gas pressure in the pressure cell at acquisition frequency of 10 times/s. At the same time, open the inlet end valve to charge CH_4. When reaching the preset gas pressure of 1.5 MPa, close the inlet end valve. (6) After 24 h of sorption, open all 6 solenoid valves to unload the gas pressure, store the test data and the coal sample image, and proceed to the next set of experiment.

3. Results and Discussion

The external conditions of this experiment are basically the same, so the difference of the data can be attributed to the change of the basic characteristics of the coal samples themselves. The relationship between the strain of the coal sample and the time is characteristic of the evolution of gas sorption-sudden unloading process, which is directly reflected in the axial strain and the radial strain.

3.1. Experimental Results. In the experiments, based on the acquired axial and radial strains, the related volumetric strain can be calculated according to the equation [38]:

$$\varepsilon_v = \varepsilon_z + 2\varepsilon_r, \tag{1}$$

where ε_v, ε_z, and ε_r are the volumetric strain, axial strain, and radial strain, respectively.

Figure 5 shows the changes in volumetric strain of the coal sample with time during the experiment, where the positive ordinate value represents shrinkage deformation and negative value represents expansion deformation. At the same gas pressure, the trend of deformation curves of different coal samples is roughly the same and could be divided into three stages. Stage I is the so-called pressure-increase-induced compression stage. In this stage, gas pressure increases with the high-pressure gas filling into the pressure cell, the pores and fractures inside the coal sample are squeezed by the external pressure, and the coal matrix shrinks inward, causing the shrinkage of the coal samples.

Stage II is the so-called sorption-induced expansion stage. In this stage, sorption-induced expansion is the dominated deformation form of the coal sample and gas undergoes seepage and sorption in the internal pore-fracture structure of the coal sample. Under the action of pressure gradient, gas

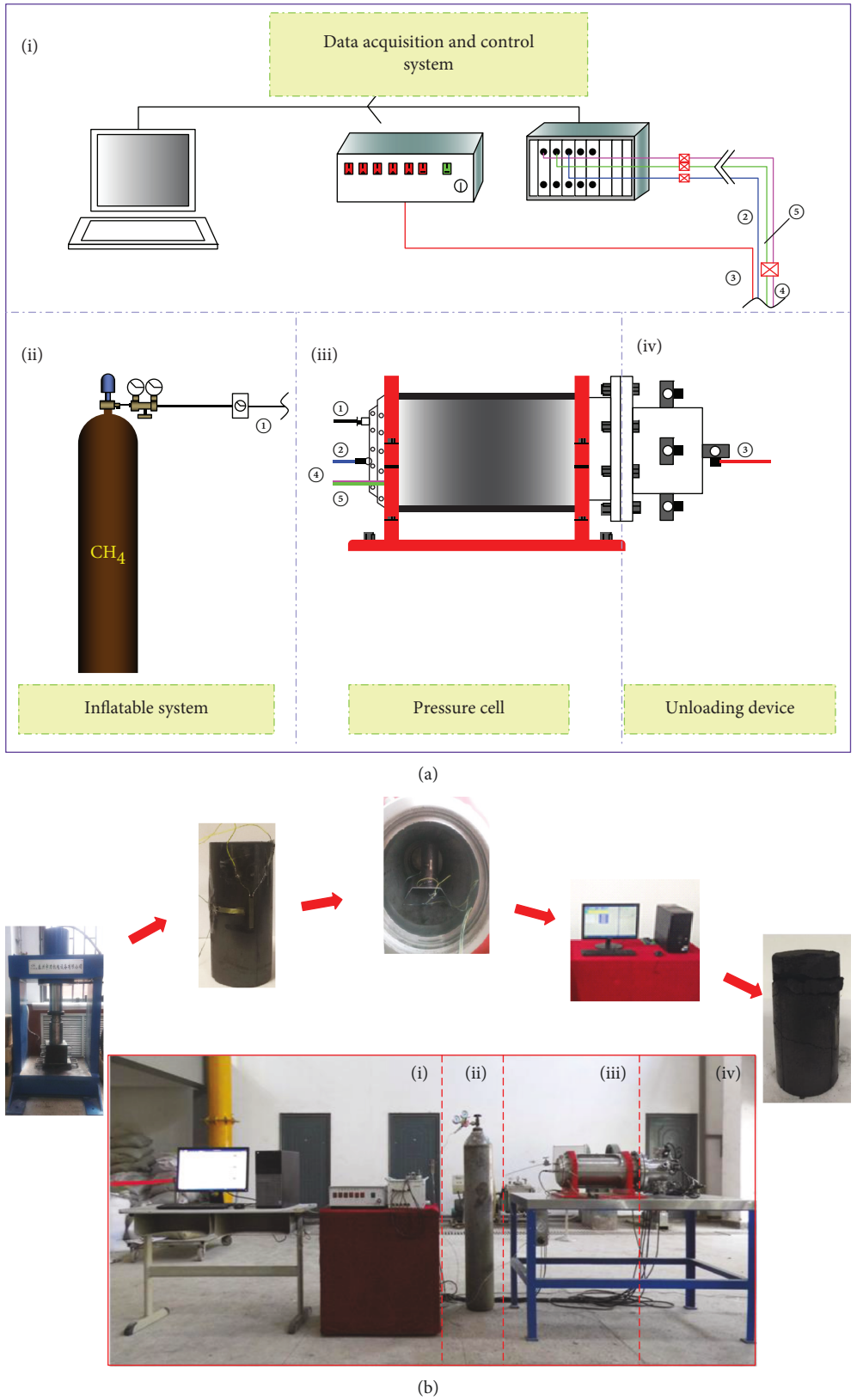

Figure 4: The schematic and operation steps of experimental system for sudden unloading of gas-bearing coal samples. (a) Schematic of the system principle: ① air-conducting tube, ② gas pressure detector, ③ solenoid valve, ④ strain gauge 1, and ⑤ strain gauge 2. (b) Apparatus system and its operation steps.

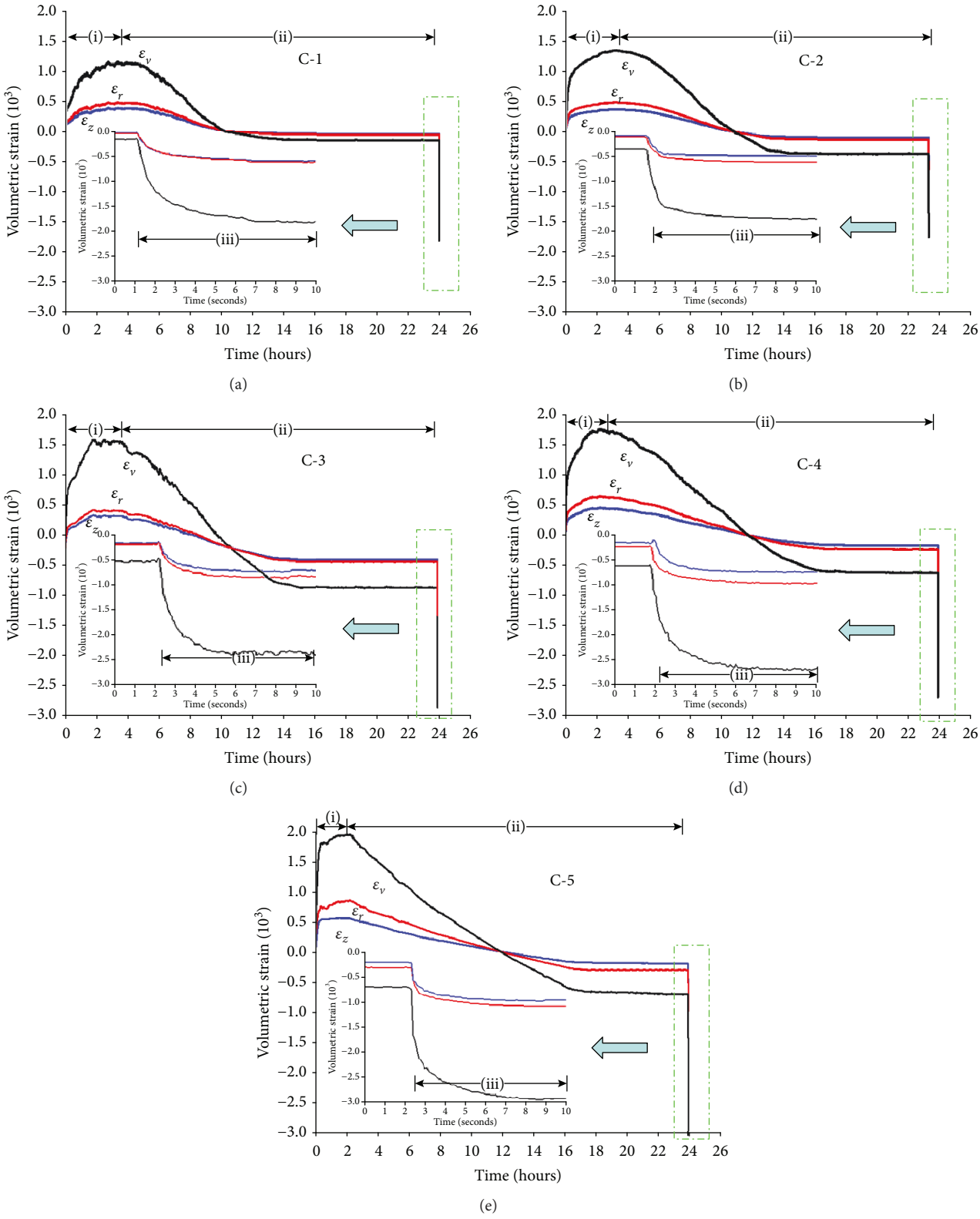

Figure 5: Development of strains (ε_r, ε_z, and ε_v) induced in coal samples during sorption-sudden unloading of methane.

molecules rapidly enter into the larger pores via seepage, continuously seep and diffuse into the interior of the coal sample, and further contact and adhere to the surface of the micropores of the coal medium. The sorption of gas decreases the surface energy of coal medium and the attraction among coal molecules, resulting in coal medium to expand and deform. Over time, these decreases gradually attenuate, and the surface energy of coal medium and the attraction among coal

molecules eventually become stable, reaching a dynamic equilibrium state of sorption-desorption.

Stage III is the sudden-unloading-induced deformation or failure stage, where the gas pressure is suddenly unloaded and the gas inside the coal under high pressure difference rapidly bursts into the surrounding environment through the seepage-diffusion effect, causing pores and cracks in the coal to expand and eventually leading to rapid deformation and failure of the coal sample. Within 2 s of the pressure unloading, about 80% of the coal samples undergo deformation. After sudden gas pressure relief, gas inside the coal rapidly bursts into the surrounding air. When reaching the equilibrium, coal sample no longer undergoes deformation.

3.2. Differences in Strain of Coal Samples with Different Pore Structures due to Gas Sorption-Sudden Unloading. Figure 6 shows the maximum compressive deformation and maximum expansion deformation of the coal sample during the experiment. Let ε_v', ε_r', and ε_z' denote the maximum compressive volume strain, radial strain, and axial strain, respectively, and ε_v'', ε_r'', and ε_z'' represent the strain after pressure unloading. It can be seen that at constant external pressure, as the particle size of the coal sample decreases, the deformation of the coal sample gradually increases. For example, the ε_v' are 1092, 1346, 1605, 1742, and 1850 for C-1 to C-5, respectively. After the sudden unloading of the pressure, at constant strain, ε_v'' reaches 1812, 2142, 2403, 2601, and 2751 for C-1 to C-5, respectively, showing smaller increase than ε_v' among different samples with particle size decreasing. Moreover, the radial strain is always greater than the axial strain for coal samples at all stages. Although the trend of changes in the axial strain and radial strain is similar, the difference between the two gradually increases with the particle size of coal sample decreasing.

Methane exists in both free and adsorbed forms in coal. The gas entering the coal sample is mainly the free gas within the macroscopic cracks inside the coal body, which plays a role in expanding the coal volume and reducing the density of coal. The continuous flow of high-pressure airflow promotes the formation of new cracks and the expansion of primary cracks in coal, accelerating the unstable failure of coal. When the coal adsorbs gas, gas molecules can be wedged between the macromolecules of a diameter equivalent to the gas molecules, so that the coal body has microscopic fractures along the coal matrix. When coal adsorbs gas, the tension on the surface of the pore and fracture decreases, resulting in a decrease in the attraction between the coal molecules and a weakening of the matrix-constrained coal molecular capacity, thus causing the coal matrix to expand and deform. Macroscopically, the cohesive force between the coal particles is reduced, and eventually the force and energy causing coal instability is reduced.

3.3. Kinetics of Sorption-Sudden Unloading. The amount of CH_4 sorption under the standard condition due to gas pressure change under constant temperature (25°C) was calculated according to the state equation of ideal gas:

$$Q = \frac{\Delta P V_s T_0}{P_m T_1}, \tag{2}$$

where Q is the amount of CH_4 sorption in coal sample in equilibrium, mL; ΔP is the difference in pressure before and after gas sorption, MPa; V_s is the free space volume after removing the coal sample, mL; T_0 is the temperature under standard condition, K; P_m is standard atmospheric pressure, MPa; and T_1 is room temperature, K.

Figure 7 shows the curve of gas sorption kinetics. The duration of the sorption-desorption is different for each sample, but the scale on the time axis in the plots is nearly the same. The rate of gas sorption is highest at the beginning of each test and remains significant in the later stages, but the relative increment in accumulated gas gradually falls. Within 3 h, the gas sorption capacity increases almost at the same rate, indicating that at this stage, the process is independent of pore structure. After that, the increase of gas sorption capacity gradually slows down and shows obvious differences among the 5 samples. In the first 6 h of the test, the deformation degree of coal samples reaches more than 80%. Moreover, the gas sorption capacity gradually increases to 14.52, 15.71, 16.47, 17.22, and 17.96 $mL \cdot g^{-1}$ from C-1 to C-5, respectively. In addition to the amount of gas sorption, the time for each coal sample to reach the sorption equilibrium is also different and gradually prolongs from C-1 to C-5.

When reaching the preset sorption time, gas pressure is quickly unloaded, and the deformation of the coal sample is shown in Figure 8. At the beginning, the coal sample undergoes large expansion deformation, showing most deformation in the first 2 s. The smaller the particle size of the test sample is, the larger the deformation.

It can be seen from Figures 7 and 8 that the deformation of coal sample has a positive correlation with the kinetics of gas sorption. Because the external conditions (temperature, pressure) of the test are almost the same, the difference in the strain of coal sample is mainly affected by the amount of gas sorption, in consistence with a previous study [39]. Under the same test conditions such as pressure and temperature, the only factor affecting gas sorption capacity is the pore structure of the coal sample. Coal is a dual-porosity reservoir, consisting of microporous matrix and macroporous cleats. As part of the coal matrix, both the micropores and transition pores are the main sites for gas sorption and the channel for gas diffusing from the matrix to the fracture system, while mesopores and macropores with a pore diameter > 100 nm constitute percolation passages for gas and water in coal. The more pores for gas seepage in the coal, the more gas molecules entering the coal. As shown in Figure 3, the smaller coal particles are more prone to gas sorption, which clearly explains why the coal with smaller particles suffers more deformation during the experiment.

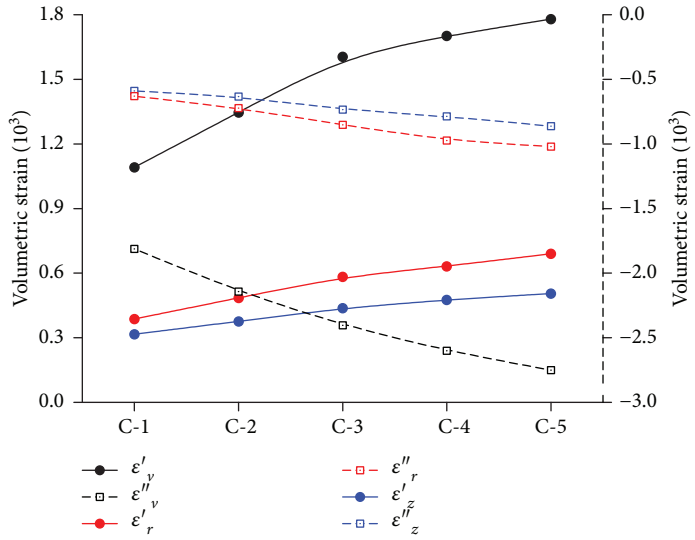

Figure 6: Maximum compressive deformation and maximum expansion deformation.

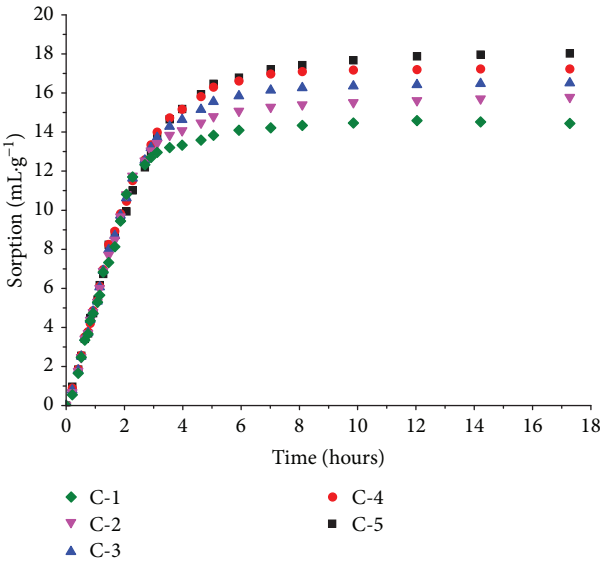

Figure 7: Kinetics of gas sorption for coal samples.

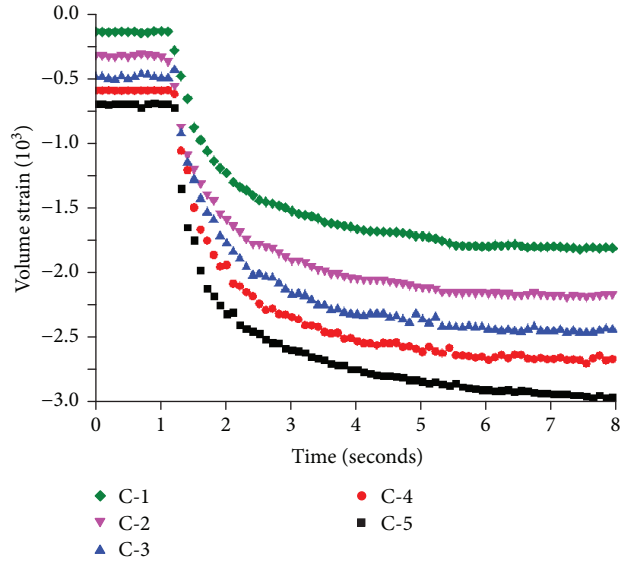

Figure 8: Volumetric strain as a function of time at sudden unloading of methane.

3.4. Analysis of Damage Characteristics of Coal Samples. As shown in Figure 9, at gas pressure of 1.5 MPa, different coal samples suffer different failure modes. At the end of the experiment, in addition to cracks, these samples have many fine fissures cracks, as shown in the yellow frame in Figure 9(a), and these fine fissures are more obvious at the upper end of each coal sample, showing obvious disintegration and destruction. This phenomenon is the so-called coal peeling. When the particle size is 0.18–0.38 mm, only four obvious cracks appear on the surface of the coal sample and the cracks at the upper end are more obvious. In addition to the cracks, the coal sample also has a relatively obvious disintegration at the edge (Figure 9(b)). For example, a large number of cracks of different sizes appear on the surface of the sample C-5. Among them, two large cracks run through the coal sample and the other small cracks interlace, extend, and expand. Besides, some coal particles obviously fall off the coal sample. Although more small cracks appear along the edge of the upper end of the coal sample, sample C-5 is still relatively tight without obvious damage (Figure 9(e)).

For samples C-2 and C-4 that have mixed coal size, in addition to some small cracks, sample C-2 also has large cracks on its surface along the axial direction and some coal particles falling off its upper end, but no crack running through it. By contrast, sample C-4 has many cracks connecting to each other with one of which running through it and two large cracks at its upper end connect to each other without causing obvious damage.

Overall, Figure 9 shows that as the particle size of the coal sample decreases, the number of cracks on its surface and

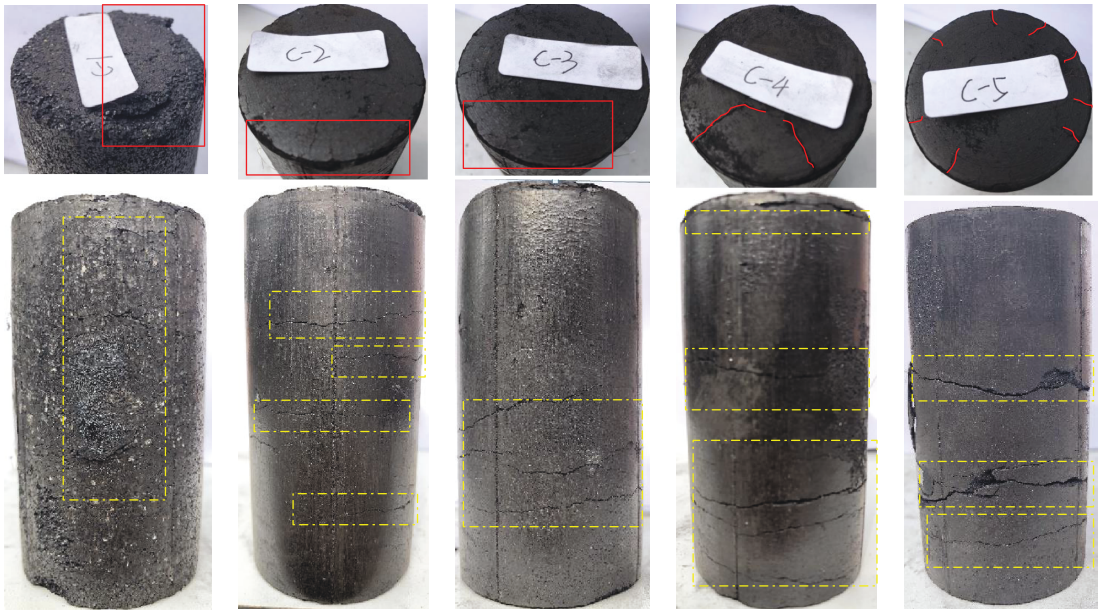

(a) (b) (c) (d) (e)

Figure 9: Failure characteristics of coal samples.

running through it gradually increases. In addition, the damage texture is along the axial direction of the coal sample, which is consistent with the experimental data showing that the radial strain is greater than the axial strain (Figure 5).

Table 1 shows that as the particle size decreases, the specific surface area of the coal sample gradually increases. It is obvious that such a phenomenon is mainly related to the specific surface area of the sample because in the process of seepage, with the injection of high-pressure gas into the coal sample chamber, coal medium with excessively large specific surface area adsorbs more gas. The sorption expansion of coal mass reduces the number effective seepage channels. In addition, the molecular layer of gas on the seepage channel also hinders the gas flow to some extent, which also reduces the number of the effective seepage channels. The larger the specific surface area, the larger the area of the coal matrix contacting gas molecules, the more the seepage channels, and the more the gas can be adsorbed. If the specific surface area is small, the coal matrix is unable to fully contact gas molecules. Thus, the amount of gas sorption is also small. Therefore, the damage of the coal sample is gradually deepened after the experiment.

4. Conclusions

In this report, we studied the influence of pore structure of coal samples on deformation of gas-bearing coals using a self-developed sudden unloading apparatus and coal briquettes with different particle sizes and reach the following conclusions. (1) The deformation of coal samples in the whole process of sorption-sudden unloading can be divided into three stages, including a pressure-increase-induced compression stage, a sorption-induced expansion stage, and a sudden-unloading-induced deformation or failure stage. (2) During the sorption-sudden unloading process, the deformation degree of samples gradually increases with sample diffusion pores and specific area increasing, and the damage degree of each coal sample shows the same changing trend. (3) The radial strain is always greater than the axial strain, and the damage of coal samples is mainly along the axial direction, rarely along the radial direction. (4) Under the same temperature, sorption pressure, and sorption time, different coal samples have different gas sorption capacity and degree of deformation during the experiments, which is related to the number of diffusion pores and specific surface areas of the coal samples.

Data Availability

The data used to support the findings of this study are available from the corresponding author upon request.

Conflicts of Interest

The authors declare that they have no conflicts of interest.

Acknowledgments

The authors gratefully acknowledge the financial supports by the National Natural Science Foundation of China (Project no. 51674158 and Project no. 51704187) as well as the Source Innovation Program (Applied Research Special-Youth Special) of Qingdao (Project no. 17-1-1-38-jch), the Shandong University of Science and Technology Research Fund (Project no. 2015JQJH105), the Taishan Scholar Talent Team Support Plan for Advantaged & Unique Discipline Areas, and the Natural Science Foundation of Shandong Province (ZR2017BEE054).

References

[1] W. Cheng, Z. Liu, H. Yang, and W. Wang, "Non-linear seepage characteristics and influential factors of water injection in gassy seams," *Experimental Thermal and Fluid Science*, vol. 91, pp. 41–53, 2018.

[2] W.-M. Cheng, X.-M. Hu, Y.-Y. Zhao, M.-Y. Wu, Z.-X. Hu, and X.-T. Yu, "Preparation and swelling properties of poly(acrylic acid-co-acrylamide) composite hydrogels," *E-Polymers*, vol. 17, no. 1, 2017.

[3] G. H. Ni, Z. Li, and H. C. Xie, "The mechanism and relief method of the coal seam water blocking effect (WBE) based on the surfactants," *Powder Technology*, vol. 323, pp. 60–68, 2018.

[4] P. Chen, E. Wang, J. Ou, Z. Li, M. Wei, and X. Li, "Fractal characteristics of surface crack evolution in the process of gas-containing coal extrusion," *International Journal of Mining Science and Technology*, vol. 23, no. 1, pp. 121–126, 2013.

[5] Q. T. Hu and G. C. Wen, *Mechanical Mechanism of Coal and Gas Outburst Process*, Science Press, Beijing, China, 2013.

[6] R. D. Lama and J. Bodziony, "Management of outburst in underground coal mines," *International Journal of Coal Geology*, vol. 35, no. 1-4, pp. 83–115, 1998.

[7] R. Lama and A. Saghafi, *Overview of Gas Outbursts and Unusual Emissions*, Third Australasian coal operators, 2002.

[8] B. B. Beamish and P. J. Crosdale, "Instantaneous outbursts in underground coal mines: an overview and association with coal type," *International Journal of Coal Geology*, vol. 35, no. 1-4, pp. 27–55, 1998.

[9] M. B. Díaz Aguado and C. González Nicieza, "Control and prevention of gas outbursts in coal mines, Riosa–Olloniego coalfield, Spain," *International Journal of Coal Geology*, vol. 69, no. 4, pp. 253–266, 2007.

[10] X. Z. Li and A. Z. Hua, "Prediction and prevention of sandstone-gas outbursts in coal mines," *International Journal of Rock Mechanics and Mining Sciences*, vol. 43, no. 1, pp. 2–18, 2006.

[11] J. Shepherd, L. K. Rixon, and L. Griffiths, "Outbursts and geological structures in coal mines: a review," *International Journal of Rock Mechanics and Mining Sciences & Geomechanics Abstracts*, vol. 18, no. 4, pp. 267–283, 1981.

[12] L. Wang, Y.-p. Cheng, C.-g. Ge et al., "Safety technologies for the excavation of coal and gas outburst-prone coal seams in deep shafts," *International Journal of Rock Mechanics and Mining Sciences*, vol. 57, pp. 24–33, 2013.

[13] S. G. Wang, D. Elsworth, and J. S. Liu, "Mechanical behavior of methane infiltrated coal: the roles of gas desorption, stress level and loading rate," *Rock Mechanics and Rock Engineering*, vol. 46, no. 5, pp. 945–958, 2013.

[14] F. H. An and Y. P. Cheng, "An explanation of large-scale coal and gas outbursts in underground coal mines: the effect of low-permeability zones on abnormally abundant gas," *Natural Hazards and Earth System Sciences*, vol. 14, no. 8, pp. 2125–2132, 2014.

[15] S. Hol, C. J. Peach, and C. J. Spiers, "Effect of 3-D stress state on adsorption of CO_2 by coal," *International Journal of Coal Geology*, vol. 93, pp. 1–15, 2012.

[16] I. Langmuir, "The constitution and fundamental properties of solids and liquids," *Journal of the Franklin Institute*, vol. 183, no. 1, pp. 102–105, 1917.

[17] Y. Li, *Comparative Research on Deformation Law of Sorption-Desorption of Briquettes and Coal Samples*, Chongqing University, Chongqing, China, 2012.

[18] X. He, E. Wang, and H. Lin, "Mechanism of pore gas deformation and erosion on coal," *Journal of Chinese University of Mining and Technology*, vol. 25, no. 1, pp. 6–11, 1996.

[19] S. N. Zhou, *Coal Gas Occurrence and Flow Theory*, Coal Industry Press, Beijing, China, 1999.

[20] H. Gao, M. Nomura, S. Murata, and L. Artok, "Statistical distribution characteristics of pyridine transport in coal particles and a series of new phenomenological models for overshoot and nonovershoot solvent swelling of coal particles," *Energy & Fuels*, vol. 13, no. 2, pp. 518–528, 1999.

[21] C. Ö. Karacan, "Heterogeneous sorption and swelling in a confined and stressed coal during CO_2 injection," *Energy & Fuels*, vol. 17, no. 6, pp. 1595–1608, 2003.

[22] C. Ö. Karacan, "Swelling-induced volumetric strains internal to a stressed coal associated with CO_2 sorption," *International Journal of Coal Geology*, vol. 72, no. 3-4, pp. 209–220, 2007.

[23] A. L. Goodman, R. N. Favors, M. M. Hill, and J. W. Larsen, "Structure changes in Pittsburgh no. 8 coal caused by sorption of CO_2 gas," *Energy & Fuels*, vol. 19, no. 4, pp. 1759-1760, 2005.

[24] B. Nie, X. Li, Y. Cui, and H. Lu, *Theory and Application of Coal Gas Migration*, Science Press, Beijing, China, 2014.

[25] R. M. Barrer, *Diffusion in and through Solid*, Cambridge University Press, 1951.

[26] J. D. St. George and M. A. Barakat, "The change in effective stress associated with shrinkage from gas desorption in coal," *International Journal of Coal Geology*, vol. 45, no. 2-3, pp. 105–113, 2001.

[27] Y. W. Ju, B. Jiang, Q. L. Hou, Y. J. Tan, G. L. Wang, and W. J. Xiao, "Behavior and mechanism of the adsorption/desorption of tectonically deformed coals," *Chinese Science Bulletin*, vol. 54, no. 1, pp. 88–94, 2009.

[28] Y. B. Liu, *Study on the Deformation and Damage Rules of Gas-Filled Coal Based on Meso-Mechanical Experiments*, Chongqing University, Chongqing, China, 2009.

[29] Y. B. Liu, S. G. Cao, Y. Li et al., "Experimental study of swelling deformation effect of coal induced by gas adsorption," *Chinese Journal of Rock Mechanics and Engineering*, vol. 29, no. 12, pp. 2484–2491, 2010.

[30] Z. Zhang, S. Cao, P. Guo, and Y. Liu, "Comparison of the deformation characteristics of coal as sorption-desorption process for raw and briquette coals," *Journal of Chinese University of Mining and Technology*, vol. 43, no. 3, pp. 388–394, 2014.

[31] N. Baisheng, L. Hongqi, and L. Xiangchun, "Experimental study on the characteristic of coal deformation during gas sorption and desorption process," *Journal of China Coal Society*, vol. 40, no. 4, pp. 754–759, 2015.

[32] Z. Liu, Z. Feng, Q. Zhang, D. Zhao, and H. Guo, "Heat and deformation effects of coal during adsorption and desorption of carbon dioxide," *Journal of Natural Gas Science and Engineering*, vol. 25, pp. 242–252, 2015.

[33] L. Brochard, M. Vandamme, R. J.-M. Pellenq, and T. Fen-Chong, "Adsorption-induced deformation of microporous materials: coal swelling induced by CO_2–CH_4 competitive adsorption," *Langmuir*, vol. 28, no. 5, pp. 2659–2670, 2012.

[34] N. Mahabadi, X. Zheng, T. S. Yun, L. van Paassen, and J. Jang, "Gas bubble migration and trapping in porous media:

pore-scale simulation," *Journal of Geophysical Research: Solid Earth*, vol. 123, no. 2, pp. 1060–1071, 2018.

[35] N. Mahabadi, S. Dai, Y. Seol, T. Sup Yun, and J. Jang, "The water retention curve and relative permeability for gas production from hydrate-bearing sediments: pore-network model simulation," *Geochemistry, Geophysics, Geosystems*, vol. 17, no. 8, pp. 3099–3110, 2016.

[36] J. L. Grozic, P. K. Robertson, and N. R. Morgenstern, "The behavior of loose gassy sand," *Canadian Geotechnical Journal*, vol. 36, no. 3, pp. 482–492, 1999.

[37] B. B. Hodort, *Coal and Gas Outbrust*, Science Press, Beijing, China, 1966.

[38] Z. G. Zhang, *Study on Characteristics of Adsorption/Desorption-Induced Deformation and Its Influencing Factors*, Chongqing University, Chongqing, China, 2015.

[39] R. Sakurovs, S. Day, S. Weir, and G. Duffy, "Application of a modified Dubinin–Radushkevich equation to adsorption of gases by coals under supercritical conditions," *Energy & Fuels*, vol. 21, no. 2, pp. 992–997, 2007.